Journal of Chromatography A, 1218 (2011) 896–906

Contents lists available at ScienceDirect

Journal of Chromatography A

journal homepage: www.elsevier.com/locate/chroma

Multi-location peak parking method: An important new tool for the study of mass transfer kinetics in liquid chromatography

Fabrice Gritti, Georges Guiochon*

Department of Chemistry, University of Tennessee, 552 Buehler Hall, Knoxville, TN 37996-1600, USA

ARTICLE INFO

Article history:
Received 20 October 2010
Received in revised form 1 December 2010
Accepted 7 December 2010
Available online 24 December 2010

Keywords:
Peak parking experiments
Multi-location peak parking
Longitudinal diffusion coefficient
Mass transfer
Column axial heterogeneity

ABSTRACT

The peak parking (PP) method probes the longitudinal diffusion coefficient of a compound at a single location along the chromatographic column. We extended to a so-called multi-location peak parking (MLPP) method, in which a large number of axial locations along the column are selected in order to check the validity of the conventional PP method and to reveal possible defaults in the structure of the packed bed or pitfalls of the PP and the MLPP methods. MLPP was applied to a series of HILIC columns, including a 5.0 μm Venusil, a 3.0 μm Luna-diol, three 2.7 μm Halo, and a 1.7 μm Kinetex columns. The results demonstrate that the MLPP method may reveal local heterogeneities in the axial diffusion of small retained low molecular weight compounds along the column. Most importantly, experiments show that the sample zone should not be parked in the entrance of the column (i.e., at <1/10 th of the column length). The abrupt drop in the flow rate considerably affects the peak shape and prevents scientists from using the conventional PP method. Practical solutions to cope with that problem are proposed and their success/failure are discussed.

1. Introduction

The peak parking method was first introduced in gas chromatography by Knox and McLaren [1] when, in 1964, these authors measured the obstruction factor of packed beds. The carrier gas was nitrogen, the probe sample ethylene. The flow rate was abruptly stopped when the zone was half-way in the column and the ethylene zone allowed to diffuse along the column during a series of residence times. Due to the high diffusion coefficients of gases ($D_m \simeq 10^{-1}$ cm^2/s), the residence times were no larger than 20 min, which lead to relatively short experiments. The authors determined that the obstruction factor of beds randomly packed with non-porous spheres (porosity close to 40%) was around 0.6.

The same approach was later used in liquid chromatography in 1983 [2] and 2006, to measure the apparent axial diffusion coefficient of thiourea along columns packed with C_{18}-bonded silica particles having different surface coverages in C_{18}-bonded chains, using a mixture of methanol and water (25/75, v/v) [3]. The main difficulty was the significantly smaller diffusion coefficients in liquids than in gases ($D_m \simeq 10^{-5}$ cm^2/s), leading to large residence times, even for low molecular weights compounds, usually of the order of 8 h. Assuming a model of diffusion in a binary heterogeneous bed (inter-particle and particle volumes [4]), allowed the derivation of values of the internal obstruction factors of porous particles with different porosities. More generally, the peak parking method became a judicious strategy for the study of mass transfer kinetics in stationary phases [5]. The application of this method is straightforward in reversed phase liquid chromatography (RPLC) where the contribution of surface diffusion to the longitudinal diffusion coefficient B of the van Deemter equation is significant [6]. The peak parking method was also applied in inverse size-exclusion chromatography (ISEC), using polystyrene standard samples to distinguish between the internal and the external diffusivity of large molecular weight compounds which are partially excluded from the mesoporous volume of the particles [7]. More recently, the peak parking method was used to measure molecular diffusivities in solution for columns packed with non-porous particles after calibration measurements had been made with an empty open tube using a micro-flow HPLC system [8,9]. Thus, the peak parking method appears as an easier, more practical, and inexpensive method to measure diffusion coefficients in liquid phase than optical or spectroscopic methods. It may consume more time, but today automatic instruments can be programmed easily to carry out this stop and flow method, to run it overnight for low molecular weight compounds and over a period of three full days to provide accurate data for heavier molecules like proteins [10–12].

The peak parking method was also used to estimate sample diffusivity across porous particles [13,4,14]. To the best of our knowledge, the molecular diffusivity of neutral compounds in a single porous particle as those used in liquid chromatography was

* Corresponding author. Tel.: +1 865 974 0733; fax: +1 865 974 2667.
E-mail address: guiochon@utk.edu (G. Guiochon).

0021-9673/$ – see front matter © 2010 Elsevier B.V. All rights reserved.
doi:10.1016/j.chroma.2010.12.024

never measured accurately under linear conditions. Attempts were made to do so in microdevices, under the influence of external electrical fields and of fixed charges [15]. Such measurements were made only for proteins, under strongly non-linear conditions, the progression of a concentration shock layer being followed by refractive index-based confocal microscopy [16,17]. We determine the molecular diffusivity of insulin in columns packed with shell particles, using a diffusion model in heterogeneous packed bed to interpret the data provided by the peak parking method [11,18]. The results demonstrated that the C coefficient of the van Deemter plot is mostly accounted for by the external film mass transfer resistance, the protein diffusivity through porous shells being much faster than its transfer from the percolating moving eluent to the internal stagnant eluent. Finally, the peak parking method appears to be useful to provide estimates of the overall eddy diffusion term of chromatographic columns by applying a simple subtraction method [14,19]. The reduced longitudinal diffusion term (B/ν) and the reduced trans-particle mass transfer resistance term ($C_p\nu$) are directly derived from the peak parking method and subtracted (together with the reduced external film mass transfer resistance term, $C_f\nu$, given by the Wilson and Geankoplis correlation [20,21]) from the measured values of the reduced height equivalent to a theoretical plate (HETP). This provided an experimental proof that the reduced eddy diffusion term of columns packed with shell particles is smaller than that of columns packed with fully porous particles by half a h unit [19].

However, the peak parking method is based on an assumption that has never been checked yet, that the bed structure is axially homogeneous and that the values measured for the diffusivity are the same everywhere along the column. To check this assumption, we parked several sample zones at different locations along the column length, equally separated from the column entrance to its exit, in order to search for possible axial heterogeneities in the structure of the packed bed and/or for possible pittfalls related to the peak parking experiments. We applied the multi-location peak parking (MLPP) method to several HILIC columns including a 150 × 4.6 mm 5 μm Venusil, three 150 × 4.6 mm 2.7 μm Halo, a 100 × 4.6 mm 1.7 μm Kinetex, and a 150 × 4.6 mm 3.0 μm Luna columns.

2. Theory

The MLPP method consists in parking simultaneously a number N of sample zones along the column. For the sake of simplification, let us consider N equidistant sample zones. The column is thus divided into $N+1$ isometric segments. The location from the column entrance, z_i, of the i th sample zone is:

$$z_i = i \times \frac{L}{N+1} \tag{1}$$

where L is the column length. N consecutive injections should be performed in order to place these N sample zones at the N locations given by Eq. (1). The time lags of the first $N-1$ injections are all the same and equal to the sum of the end time of the method, t_{end}, and the time delay, t_{delay} between the end of a method to the start of the next method. The end time of the last injection method is defined by the time, t_{stop}, at which the flow rate, F_v, is abruptly stopped in order for the N concentration zones to relax simultaneously along the column. The last injection locates the sample zone at $z = z_1$. Therefore:

$$t_{stop} = \frac{1}{N+1} t_R \tag{2}$$

where t_R is the retention time of the zone that would migrate along the whole column length without being stopped (note that the extra-column time is neglected). It is written:

$$t_R = \frac{V_0}{F_v}(1+k) \tag{3}$$

where V_0 is the hold-up volume of the column and k is the retention factor of the sample. Note that a limit to t_{stop} is imposed by the retention of the sample and the number of peak parking locations chosen by the analyst.

The sample zone placed at location z_i comes from the $(N-i+1)$ th injection. Its migration along the column is stopped at time t_{N-i+1}, given by:

$$t_{N-i+1} = \frac{i}{N+1} t_R = t_{stop} + (i-1)(t_{end} + t_{delay}) \tag{4}$$

t_{delay} depends on the instrument, the sample volume, the sample drawing speed, and the time necessary for the instrument to download the injection method. Injection methods are series of experimental parameters such as the flow rate, the eluent composition, the run time, the injection volume, the oven temperature, the detection wavelength, the sampling rate, and the programmable time events, which are collected in a file that defines the experimental conditions under which an analysis is carried out. These files are implemented in the chromatographic software of the instrument. It takes a finite, significant, and measurable amount of time for the software to call an injection method before the run is started. For instance, it was measured at 36 s for a 1 μL injection using the Infinity 1290 instrument at a drawing speed of 100 μL/min.

By summing up the N Eq. (4) and after simplification, we obtain:

$$t_{end} = t_{stop} - t_{delay} \tag{5}$$

Since t_{end} is necessarily positive, a maximum flow rate $F_{v,\max}$ is defined by $t_{stop} > t_{delay}$ and

$$F_{v,\max} = \frac{V_0(1+k)}{t_{delay}(N+1)} \tag{6}$$

In conclusion, the flow rate is not set in the MLPP method (as in the traditional PP experiments) as long as it is kept smaller than $F_{v,\max}$. Once F_v is arbitrarily fixed by the analyst, the run time t_{end} of the first $N-1$ injection methods is fixed.

In addition, the maximum parking time, $t_{p,\max}$, is defined so that the sample zones 1 and N do not diffuse out of the column at its entrance and exit. If we consider the 6σ base width of these Gaussian zones, this condition translates into the following inequality:

$$3\sigma < \frac{L}{N+1} \tag{7}$$

The variance σ_N^2 of the band close to the column outlet is written:

$$\sigma_N^2 = H z_N + 2 D_{app} t_{p,\max} \tag{8}$$

where D_{app} is the apparent axial diffusion coefficient of the sample along the column. Roughly, as a first approximation, we can assume $H = 2d_p$ and $D_{app} = D_m/(\epsilon_t(1+k))$ and the maximum parking time is estimated by:

$$t_{p,\max} \simeq \frac{\epsilon_t(1+k)L}{(N+1)D_m}\left[\frac{L}{18(N+1)} - N d_p\right] \tag{9}$$

With sub-5 μm particles, assuming that there should be 10 different peak parking locations along a 10–15 cm long column, Eq. (9) simplifies to:

$$t_{p,\max} \simeq \frac{\epsilon_t(1+k)L^2}{18(N+1)^2 D_m} \tag{10}$$

To apply these theoretical results, we consider $\epsilon_t = 0.6$, $k = 1$ (moderately retained sample), $L = 15$ cm, $N = 9$ (9 peak locations), and $D_m = 1 \times 10^{-5}$ cm^2/s (diffusion coefficient of small molecules). The

arithmetic calculations show that the maximum peak parking time should be no larger than 15,000 s or about 4 h.

3. Experimental

3.1. Chemicals

The mobile phase was a mixture of water and acetonitrile (5/95, v/v). These two solvents were HPLC grade from Fisher Scientific (Fair Lawn, NJ, USA). The mobile phase was filtered before use on a surfactant-free cellulose acetate filter membrane, 0.2 μm pore size (Suwannee, GA, USA). The samples uracil and toluene were also purchased from Fisher Scientific.

3.2. Columns

The 150 × 4.6 mm 5.0 μm Venusil column (Agela Technologies, Newark, DE, USA), the three 150 × 4.6 mm 2.7 μm Halo HILIC columns (Advanced Material Technology, Wilmington, DE, USA), the 150 × 3.0 mm 3.0 μm Luna-diol and 100 × 4.6 mm 1.7 μm Kinetex columns (Phenomenex, Torrance, CA, USA) were of generously offered by their respective manufacturer. The surfaces of all particles were neat silica, except for the Luna-diol silica. All the packing materials used are suitable for use in HILIC mode. The average mesopore size is 90 Å for Halo, 100 Å for Venusil and Kinetex, and 200 Å for Luna-diol porous particles.

3.3. Multi-location peak parking measurements

The principle of the standard PP method was previously described [3]. In PP experiments, a single band is injected, eluted to some place in the column (the middle of the column is commonly chosen), parked there and left to diffuse axially for a while, after what elution is resumed. In the MLPP method, a sequence of N successive injections is performed and as many bands are parked in as many locations spread along the column. In the theory section, we elaborated on the constraint applied to the constant flow rate, which should not be larger than $F_{v,\max}$. For the experiments reported here, the time delay, t_{delay}, was measured at 36 s; the constant flow rate and the method stop time were 0.31 mL/min and 2.24 min (Venusil, 5 locations), 0.40 mL/min and 0.77 min (Venusil, 9 locations), 0.10 mL/min and 0.69 min (Luna-diol, 9 locations), 0.18 mL/min and 0.84 min (Halo HILIC, 9 locations), and 0.15 mL/min and 0.43 min (Kinetex, 9 locations). Each one of these flow rates was arbitrarily chosen, smaller than $F_{v,\max}$. For each column, the series of peak parking times set in the MLPP experiments are given in the results and discussion section.

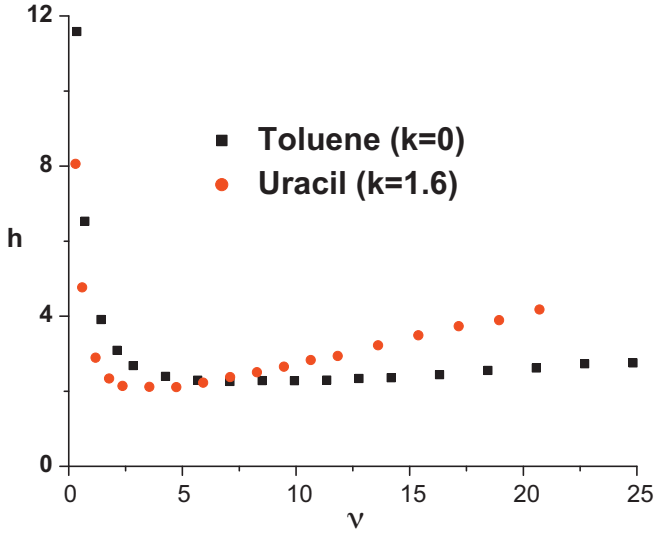

Fig. 1. Plots of the corrected reduced plate heights, h, of toluene (full squares) and uracil (full circles) versus the reduced interstitial linear velocity, ν. The column is the 150 × 4.6 mm 5 μm Venusil column. T = 295 K. The mobile phase was a mixture of acetonitrile and water (95/5, v/v). Note, in contrast to RPLC, the larger longitudinal diffusion coefficient (B coefficient in the van Deemter equation) of the unretained species (toluene) in comparison to that of the non-retained compound (uracil).

3.4. Measurement of the HETP data

The peak response of uracil and toluene were recorded at a wavelength of 259 nm. The detector bandwidth was fixed at 4 nm.

The sequence of flow rates used was 0.05, 0.1, 0.2, 0.3, 0.4, 0.6, 0.8, 1.0, 1.2, 1.4, 1.6, 1.8, 2.0, 2.3, 2.6, 2.9, 3.2. and 3.5 mL/min. The reduced velocities were derived from the diffusion coefficient of uracil and toluene in the mixture of water and acetonitrile used (5/95, v/v), according to the

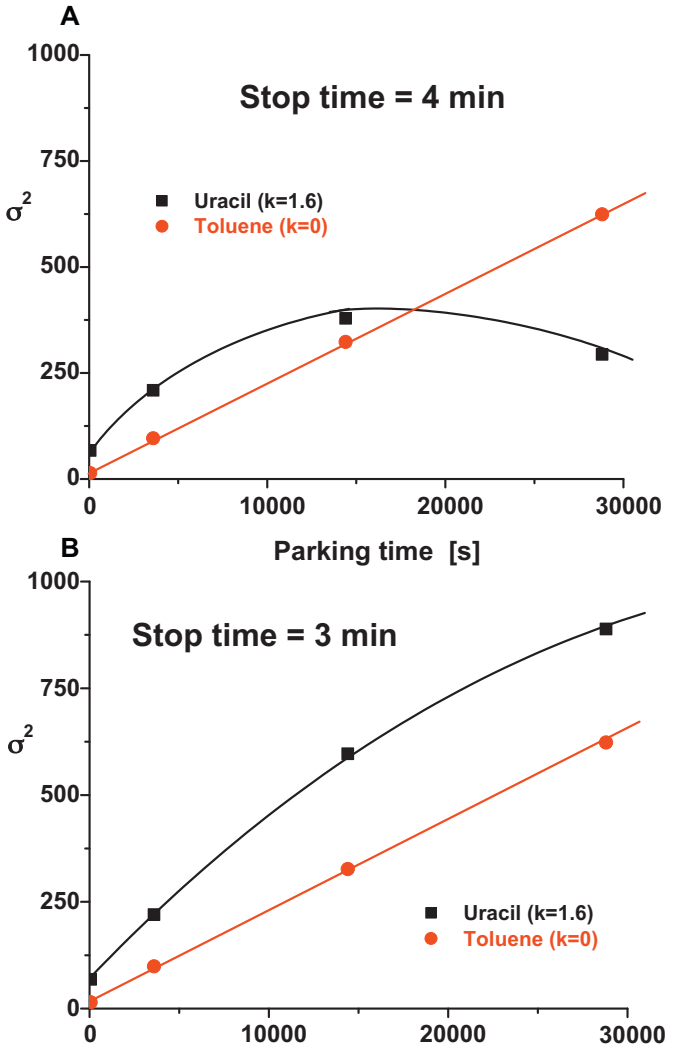

Fig. 2. Plots of the peak variances of uracil (full squares) and toluene (full circles) versus the parking times (1, 60, 240, and 480 min) measured after applying the standard (one peak location) peak parking method. Same eluent and column as in Fig. 1. T = 295 K. Flow rate : 0.3 mL/min. In the PP experiments, the flow rate was abruptly stopped after an elution time of 4 min (A) and 3 min (B). Note the unexpected deviation of the plot of uracil from linearity and the effect of the sample location in the column on the plot. At the same time, note the strictly identical plots of toluene in both (A) and (B).

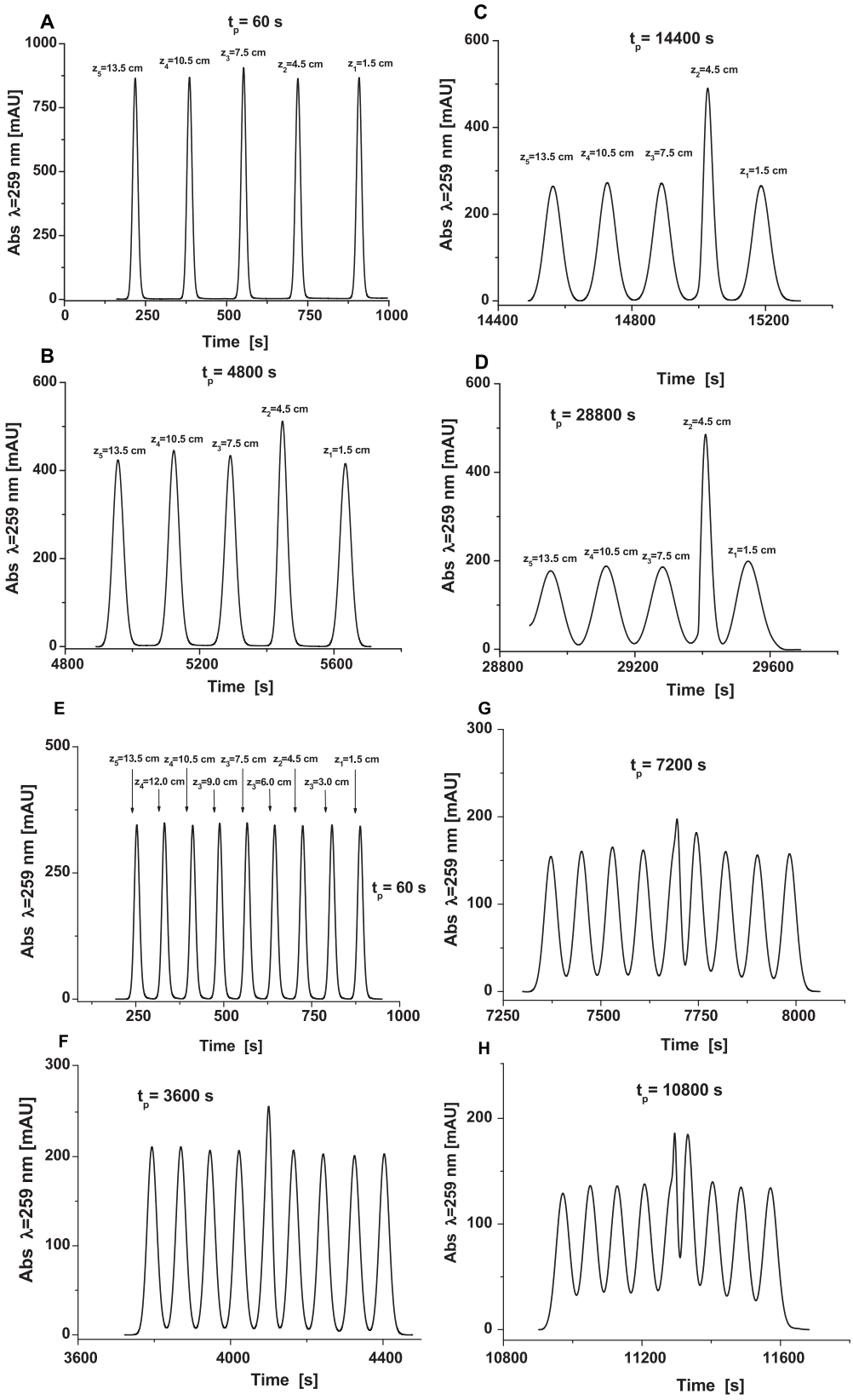

Fig. 3. Chromatograms of uracil recorded during the first MLPP experiment sequence. Same eluent, temperature, and flow rate as in Fig. 2. 5 sample locations were selected along the column as indicated in the figures. The parking times were 1 min (A), 80 min (B), 240 min (C), and 480 min (D). Note the striking anomaly in the static sample band broadening at the position $z \simeq 4.5$ cm from the column entrance. Chromatograms of uracil recorded during the second MLPP experiment sequence. Same temperature and column as in Fig. 3. The content of acetonitrile was increased from 95% to 97% in order to squeeze a larger number of peaks within the retention window. The flow rate was set as 0.4 mL/min. 9 sample locations were selected along the column as indicated in the figures. The parking times were fixed at 1 min (E), 60 min (F), 240 min (G), and 480 min (H). Note the slight shift of the band broadening anomaly to the position $z \simeq 6.5$ cm from the column entrance.

Wilke and Chang correlation [22] ($D_{m,\text{uracil}} = 2.42 \times 10^{-5}$ cm^2/s and $D_{m,\text{toluene}} = 2.16 \times 10^{-5}$ cm^2/s). Given the possible error made on the diffusion coefficient (±10%), the external porosity was assumed to be the same at $\epsilon_e = 0.43$ for all the columns tested. The external porosity of the columns packed with HILIC particles was measured by inverse size-exclusion chromatography (ISEC). It varies consistently between 0.42 and 0.44 [11]. For each of these 18 flow rates and for each sample, the extra-column contributions to the retention volume and to the overall band broadening of the probes were measured by replacing the chromatographic column with a ZDV union connector. The experimental HETP data were corrected for the contribution of the 1290 Infinity HPLC system. The extra-column and the total band variances were measured by the numerical integration method. Prior to any measurement, each profile recorded was cut on its left and right side and corrected for baseline drift. Accordingly, the first and the second central moments of the concentration profiles, calculated in an Excell spreadsheet, are given by:

$$\mu_1 = \frac{\sum_{i=1}^{i=N-1}(C_i + C_{i+1})(t_i + t_{i+1})}{2\sum_{i=1}^{i=N-1} C_i + C_{i+1}} \tag{11}$$

$$\mu_2' = \frac{\sum_{i=1}^{i=N-1}(C_i + C_{i+1})\left((t_i + t_{i+1})/(2) - \mu_1\right)^2}{\sum_{i=1}^{i=N-1} C_i + C_{i+1}} \tag{12}$$

where N is the number of data points (t_i, C_i) left after the left and right cut-off of the full recorded signal.

The corrected reduced HETP, h, is then given by:

$$h = \frac{L}{d_p}\frac{\mu_2' - \mu_{2,ex}'}{\left(\mu_1 - \mu_{1,ex}\right)^2} \tag{13}$$

where L is the column length, d_p the mean particle size, and $\mu_{1,ex}$ and $\mu_{2,ex}'$ are the first and second central moments of the corresponding extra-column band profiles.

The precision of the h data is given by

$$\left|\frac{\Delta h}{h}\right| = \left|\frac{\Delta\mu_2'}{\mu_2'}\right|\left(\frac{\mu_2' + \mu_{2,ex}'}{\mu_2' - \mu_{2,ex}'}\right) + 2\left|\frac{\Delta\mu_1}{\mu_1}\right|\left(\frac{\mu_1 + \mu_{1,ex}}{\mu_1 - \mu_{1,ex}}\right) \tag{14}$$

The second and first moments of the tracer peak, μ_2' and μ_1, were measured successively three times each, first with the chromatographic column, then with a zero-volume connector (ZDV) fitted to the instrument. The relative errors made on these moments were always less than 3 and 0.5%, for the second and the first

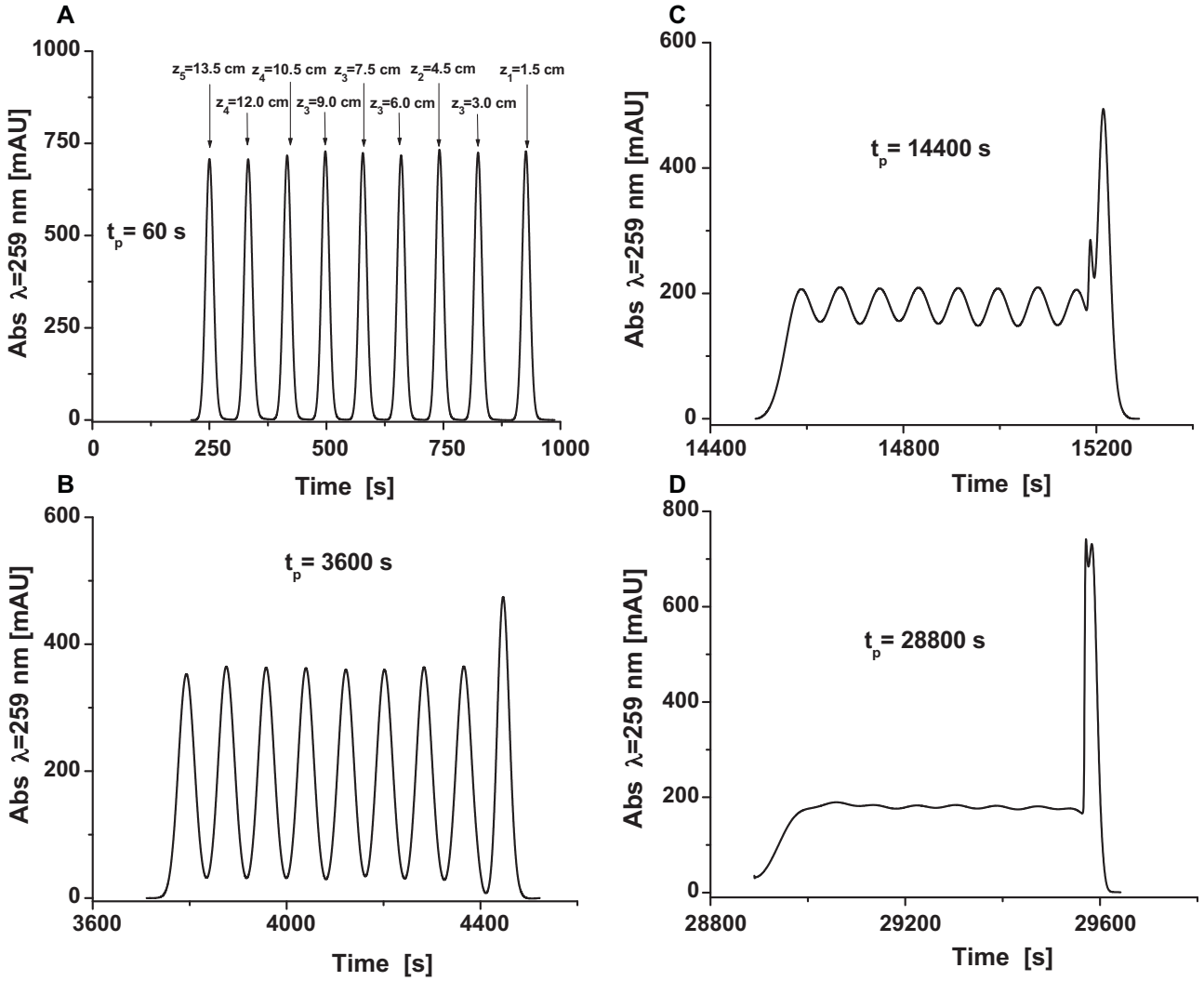

Fig. 4. Chromatograms of uracil recorded during the MLPP experiment sequence with the Halo HILIC column 1. Same eluent and temperature as in Fig. 3. The flow rate was set at 0.18 mL/min. 9 sample locations were selected along the column as indicated in the figures. The parking times were 1 min (A), 80 min (B), 240 min (C), and 480 min (D). Note the striking anomaly in the static sample band broadening at the entrance position of the column for $z \simeq 1.5$ cm.

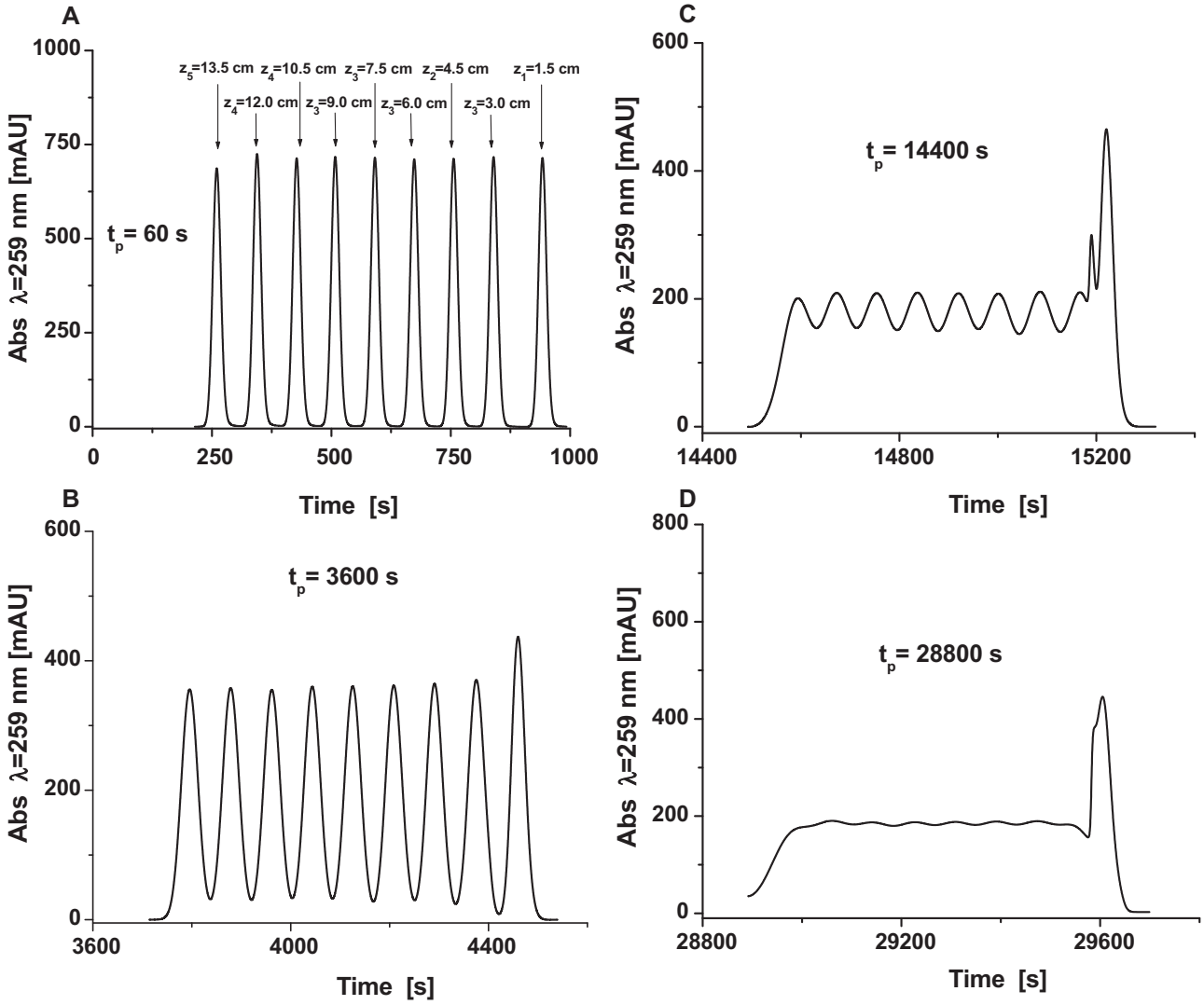

Fig. 5. Same as in Fig. 4 except the column Halo HILIC 2. Note, again, the severe anomaly on the last eluted peak.

moments, respectively.[1] The precision of the integration method depends essentially on the reproducibility of the left and right cut-off abscissa. The precision of 3% was obtained when these abscissa were strictly identical, at constant flow rate. However, from one flow rate to another, the cut-off abscissa necessarily changes, therefore, the precision of the peak variance plotted as a function of the flow rate may appear larger. Yet, this integration approach (Eq. (11)) provides the most accurate HETP data that analysts can get [23]. It is far better than that of other approximate approaches, such as the half-height peak width and/or the peak fitting methods.

Accordingly, if the extra-column contributions were negligible, the largest random error would be of the order of 4%, which is typically the case with large volume columns. This contribution affects particularly small columns. For instance, if μ'_2 is only twice $\mu'_{2,ex}$ and μ_1 about ten times $\mu_{1,ex}$, the maximum random error becomes close to 10%.

4. Results and discussion

We recently investigated the mass transfer kinetics in HILIC columns. PP experiment is an important tool that provides accurate determinations of specific mass transfer terms in chromatographic columns [14]. We first discuss measurements of the kinetic performance of the HILIC column packed with 5.0 μm Venusil particles (toluene and uracil samples) in an acetonitrile-rich eluent (acetonitrile–water mixture, 95/5, v/v). The measurement of the longitudinal diffusion coefficient B requires applying the standard PP method. We discuss the results that the PP experiments gave for this column and compare them with those of the MLPP, in order to check the validity of the initial observations for any position along the column and to extend the application to the method to three other brands of HILIC columns. Finally, we investigate the origin of some unexpected but systematic anomalies observed in MLPP experiments and conclude by recommendations on the implementation of the standard PP method in order to measure correct longitudinal diffusion coefficients.

4.1. Mass transfer resistance in the Venusil HILIC column

Fig. 1 shows the reduced HETP plots of toluene and uracil. The retention factor of uracil is 1.6 whereas toluene is not retained (hydrophobic samples are excluded from the adsorbed layer of water onto the silica surface). In contrast to what is usually observed in RPLC, the longitudinal diffusion coefficient B of the more retained compound is smaller than that of the non-retained compound. This suggests that surface diffusion is absent in HILIC

[1] Note that it is the excellent repeatability of the injection system of the 1290 Infinity system that allowed the achievement of this level of reproducibility.

mode because the nature of the silica/eluent interface in HILIC in different than that of silica-C_{18}/eluent in RPLC.

In order to confirm this important observation, standard PP experiments were carried out at a flow rate of 0.3 mL/min, with a stop time set at 4 min in the injection method. The hold-up volume V_0 of the 4.6 × 150 mm Venusil column is 1.78 mL. The peaks of the probe compounds, toluene (k = 0) and uracil (k = 1.6) were thus located at distances of 10 and 2.7 cm from the column entrance when the flow was stopped. Fig. 2A shows plots of the peak variance measured as a function of the parking time for both compounds. As expected when the variance increases linearly with increasing parking time, these plots are quasi-linear for toluene, giving a B coefficient of 3.54, in good agreement with the diffusion branch of the HETP curve. On the other hand, the plot for the retained compound uracil is not linear, suggesting virtually no axial diffusion along the column for parking times larger than 2 h. Such a surprising observation was never made before and this result appears at first glance questionable. The very same peak parking experiments were repeated two days later, in order to test the reproducibility of the measurements. The same results were obtained. They seemed to suggest that the bed structure at a distance of 3 cm from the column inlet is different from that at 10 cm. In a second series of PP experiments, the flow stop time of each experiment was decreased from 4 to 3 min. Toluene and uracil were then allowed to diffuse at locations 7.5 and 2 cm along the column, respectively. The results of this PP experiment are shown in Fig. 2B. The plot of the peak variances of toluene are barely changed but that of uracil has strikingly increased for parking times longer than 1 h, without having become really linear. A repeat of the same experiments with a stop time of 3 min confirmed the result shown in Fig. 2B. In conclusion, the anomaly observed with uracil is directly related to the position of its peak inside the column, position around which the concentration gradients are relaxed by diffusion.

Surprisingly, axial diffusion of a band may depend on its location along the column. A mere difference of 0.7 cm between the band locations in the bed is able to lead to important differences in the local diffusivity of this zone. This was when we decided to develop and use the MLPP method and to use it in order to probe simultaneously sample diffusivity at several locations.

4.2. Multi-location peak parking (MLPP) measurement

5 different peak parking locations were selected along the 15 cm long Venusil column (z = 1.5, 4.5, 7.5, 10.5, and 13.5 cm). The flow rate was set at 0.31 mL/min, with t_{end} = 2.24 min, and t_{stop} = 1.42 min. A 0.5 μL sample of a 1 g/L solution of uracil was injected and detected by UV absorption at λ = 259 nm. Fig. 3A–D shows the corresponding chromatograms for parking times of 1, 80, 240, and 480 min, respectively. Interestingly, all five eluted

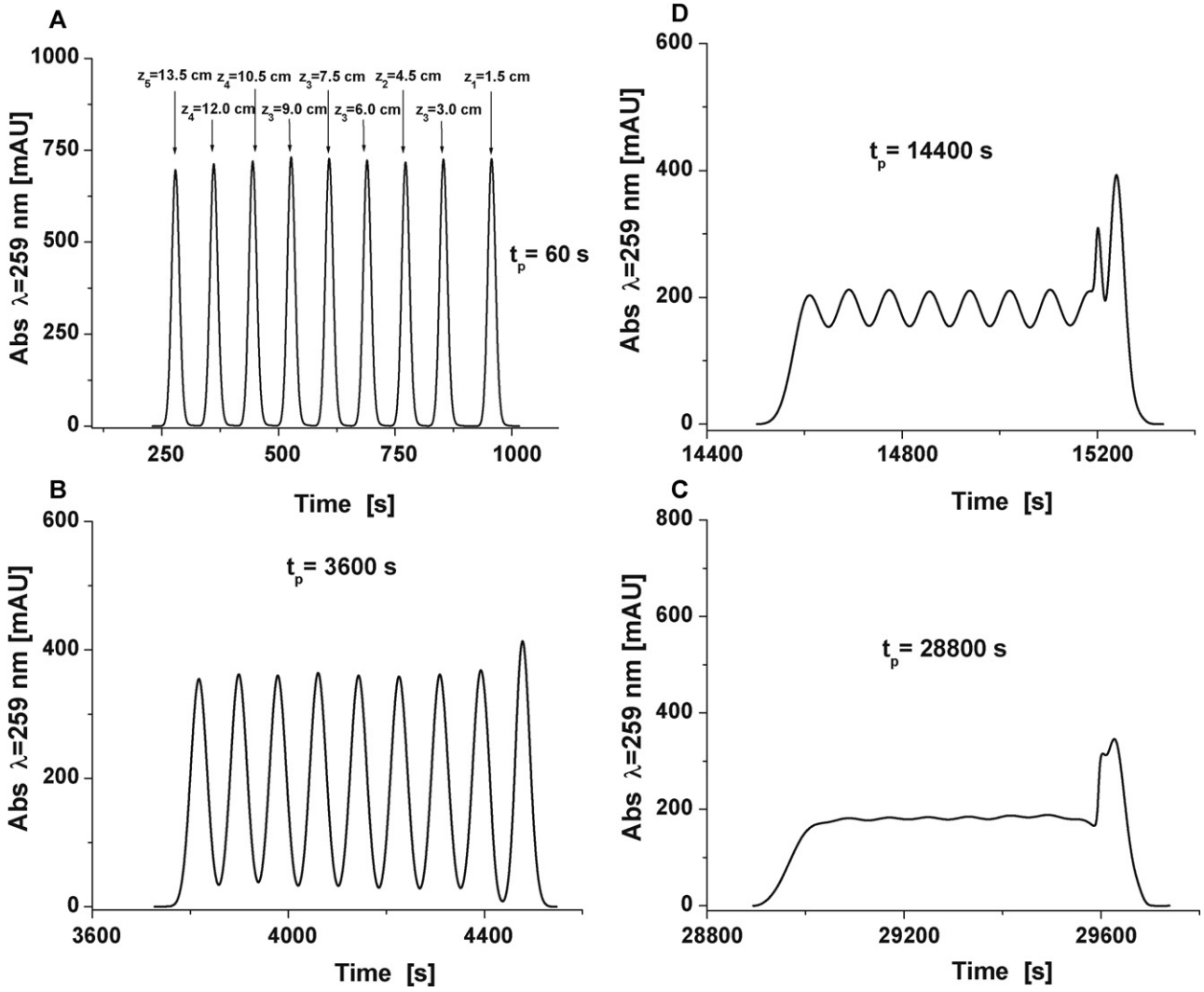

Fig. 6. Same as in Fig. 4 except the column Halo HILIC 3. Again, the band broadening of the last eluted peak is progressively distorted as the parking time increases.

peak profiles recorded are nearly undistinguishable when the flow has been stopped for only 1 min. This illustrates the high level of reproducibility of the sample volume injected by the 1290 Infinity HPLC system. However, the anomaly of axial diffusion occurring at the location $z = 4.5$ cm increases with increasing peak parking time from 80 min to 8 h. The band widths of the zones located at $z = 1.5$, 7.5, 10.5, and 13.5 cm are nearly identical, suggesting that the packed bed has the same structure in these four regions. The anomaly of band broadening detected by the MLPP experiment at the location $z = 4.5$ does not seem to be fully consistent with the result of the standard PP method, which showed an anomaly at 2.7 cm for uracil. The reason for the slight shift in the position of the anomaly is unknown, but the MLPP confirms that the longitudinal diffusion of the sample is not equivalent everywhere in the column.

A second sequence of injections (this time 9) was carried out in order to place the zones at the locations $z = 1.5$, 3.0, 4.5, 6.0, 7.5, 9.0, 10.5, 12.0, and 13.5 cm along the Venusil column. The acetonitrile concentration was increased to 97% in order to increase the retention factor of uracil to $k = 2.06$, permitting the accurate parking of up to 9 zones along the column. The flow rate was set at 0.40 mL/min, with $t_{end} = 0.77$ min, and $t_{stop} = 1.37$ min. The peak parking times were selected at 1, 60, 120, and 240 min. The results are shown in Fig. 3E–H. Interestingly, the position of the anomaly appears to have shifted again, this time from 4.50 to 5.25 cm. Everywhere else, the rate of the band spreading is nearly the same.

This series of measurements demonstrate that the MLPP results are more important than those of the standard PP method, characterize better the bed homogeneity, and permit the detection of isolated zones along the column where axial diffusion is different from elsewhere in the column. Next, we applied the MLPP method to other brands of HILIC columns (Halo, Kinetex, and Luna-diol).

4.3. Application of the MLPP method to other HILIC columns

The same MLPP measurements were made for the five other HILIC columns. The goal was to check whether anomalies similar to those observed in the Venusil column and reported in the previous section occur also in a number of commercially available HILIC columns.

4.3.1. 4.6 × 150 mm columns packed with 2.7 μm Halo HILIC

Three Halo HILIC columns (4.6 × 150 mm) were tested. Two were packed with the same batch of particles (columns 1 and 2, packing lot AHF0858) while the third column was packed with a different lot (column 3, packing lot AHF0738). Nine different locations were selected along these columns, at $z = 1.5$, 3.0, 4.5, 6.0, 7.5, 9.0, 10.5, 12.0, and 13.5 cm. The flow rate was set at 0.18 mL/min, with $t_{end} = 0.84$ min, and $t_{stop} = 1.45$ min. Figs. 4A–D, 5A–D, and 6A–D show the MLPP results for columns 1, 2, and 3, respectively. It is noteworthy that the chromatograms obtained for these three columns are very similar. The packing process used provides a high level of column-to-column reproducibility. However, a systematic anomaly in the sample diffusion is detected at around 1.5 cm from the column entrance. Similarly to the observation made with the Venusil column, axial diffusion is highly restricted in this region and band broadening does not take place in this very location in the column.

4.3.2. 4.6 × 100 mm columns packed with 1.7 μm Kinetex HILIC

In this case, the MLPP flow rate was set at 0.15 mL/min, with $t_{end} = 0.43$ min, and $t_{stop} = 1.03$ min. Three parking times were selected at 1, 60, and 240 min. The sample zones were parked at $z = 1$, 2, 3, 4, 5, 6, 7, 8, and 9 cm. The chromatograms are shown in Fig. 7A–C. As for the Halo columns, we observe the same hindrance to axial diffusion at the entrance of the column, around $z = 1$ cm but this effect is lesser. Note also in Fig. 7B, that the valley between two consecutive peaks becomes gradually deeper from the outlet to the inlet of the column. This suggests a progressive reduction in the rate of axial diffusion as the band migrates from the entrance of the column to its exit.

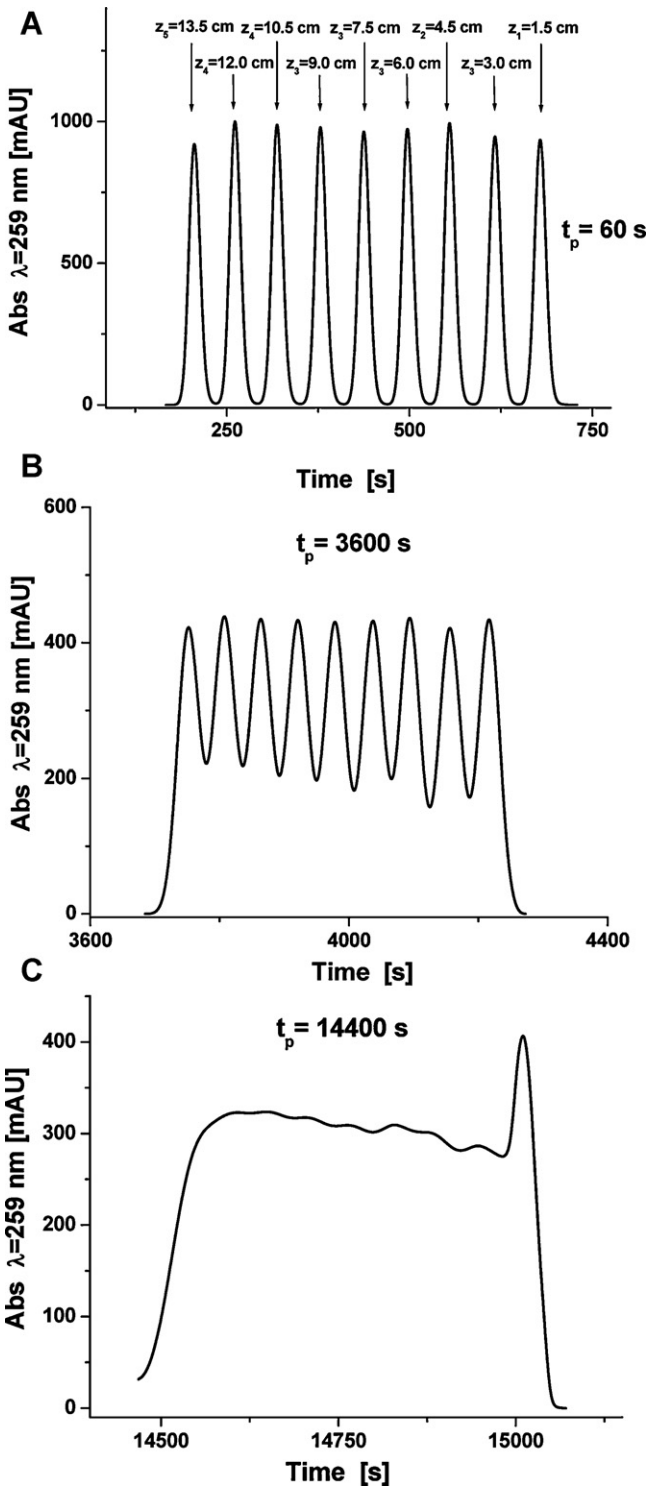

Fig. 7. Chromatograms of uracil recorded during the MLPP experiment sequence with the Kinetex HILIC column. Same eluent and temperature as in Fig. 3. The flow rate was set at 0.15 mL/min. 9 sample locations were selected along the column as indicated in the figures. The parking times were 1 min (A), 60 min (B), and 240 min (C). The same anomaly as in Figs. 4–6 is observed with the Kinetex column.

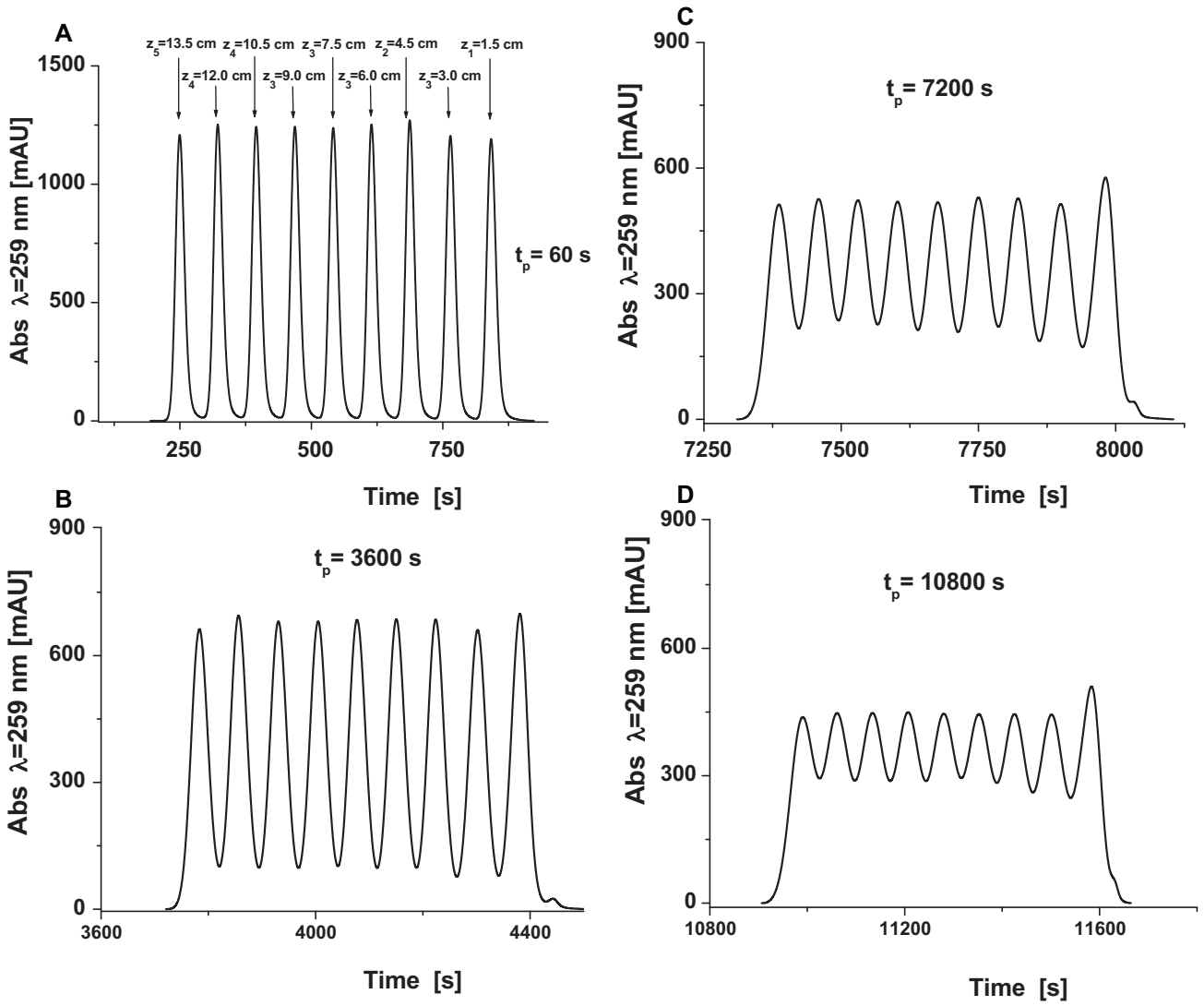

Fig. 8. Chromatograms of uracil recorded during the MLPP experiment sequence with the Luna-diol column. Same eluent and temperature as in Fig. 3. The flow rate was set at 0.10 mL/min. 9 sample locations were selected along the column as indicated in the figures. The parking times were 1 min (A), 60 min (B), 120 min (C), and 240 min (D). The same anomaly as in Figs. 4–7 is observed with the Luna-diol column.

4.3.3. 3.0 × 150 mm columns packed with 3.0 μm Luna-diol HILIC

The same MLPP experiments as those described earlier were repeated with this fourth brand of HILIC columns. The flow rate was set at 0.10 mL/min, with t_{end} = 0.69 min and t_{stop} = 1.29 min. The retention factor k of uracil is 0.9. The results of the MLPP method are shown in Fig. 8A–D. The peak parking times were set at 1, 60, 120, and 180 min. The sample zones were located at z = 1.5, 3.0, 4.5, 6.0, 7.5, 9.0, 10.5, 12.0, and 13.5 cm. No severe anomalies were observed at any position along the Luna column. Yet again, it is clear that the sample diffusivity is reduced at the entrance of the column for z = 1.5 cm (see Fig. 8D).

In conclusion, the analysis of the results observed in Section 4.1 (Fig. 3D), Section 4.3.1 (Figs. 4C, 5C, and 6C), Section 4.3.2 (Fig. 7C), and Section 4.3.3 (Fig. 8D) demonstrates altogether that:

(1) The MLPP method allows the detection of isolated spots along a column where longitudinal diffusion is slower, possibly because more hindered than in most of the rest of the column. The effect becomes most important at large peak parking times (see Fig. 3D for the most striking result).
(2) The anomalies observed by MLPP may not be related to local structural defaults in the packed bed. The results shown in Fig. 3D and H demonstrate that the location of the band broadening anomaly may vary over time when MLPP experiments are repeated with a different number of locations, 5 (Fig. 3D) and 9 (Fig. 3H).
(3) The closer to the column entrance the zone is parked, the more significant the perturbation of the axial diffusion of the band. Band diffusion seems to be severely hindered in this part of the column. Even more surprising, in the case of the Halo HILIC column 1 (Fig. 4D), the height of the zone at z = 1.5 cm increases with increasing parking time, suggesting that uracil accumulates and is concentrated in this region of the column. The cause of this phenomenon is unknown. A first element of answer is discussed in the next section.

4.4. Eliminating the anomalies taking place in the MLPP experiments

Admittedly, we do not have any satisfactory answer regarding the origin of the anomalies observed in the PP and MLPP experiments reported. These distortions could be due to a physical blockage caused by the presence of air bubbles. Poor mesopore wetting after the pressure is released could be at the origin of

this problem. Yet, the contact angles of water and acetonitrile are both smaller than 5° C [24] on bare silica surfaces, therefore these solvents wet the mesopore surface area instantaneously. Additionally, the mobile phase was carefully degassed in all our experiments. The low solubility of uracil could explain its local precipitation, which would also justify the peak anomalies. Yet, if this were true, the problem would spread everywhere along the column, not just at specific locations as observed in this work. Also, uracil was dissolved in the mobile phase and no precipitation was observed in the sample vial. These results are shocking. For the time being, they prevent scientists from using the standard one location PP method for the experimental determination of longitudinal diffusion coefficients in chromatographic columns. This would expose them to the risk of positioning the band in a location where unexpected anomalies in band broadening take place.

Our most striking observation is that we have never so far obtained MLPP results in which there was no anomaly, despite having tested six different columns. This cannot be a coincidence. These results must have a rational, scientific explanation. We suggest that the anomalies observed are not due to the column itself and a hypothetical structural default in the packed bed but rather by the nature of the peak parking protocol. The common feature between the standard PP and the MLPP experiments is that the flow rate is abruptly stopped (before static diffusion begins) then abruptly resumed (ending the static diffusion step). The constant flow rate used in PP experiments is not large (usually between 0.10 and 0.40 mL/min with conventional analytical columns), yet the sudden decrease and increase of the inlet pressure can perturb significantly the band profiles because the eluent has a finite compressibility and a pressure shock propagates when the flow rate stops abruptly. This shock (ca. 50 bar) relaxes progressively but a finite time is required before the pressure becomes constant all along the column. A similar, converse phenomenon takes place when the flow rate is resumed and the pressure gradient along the column builds up progressively along the whole column. Consequently, the local velocity vary along the column during both transient phases and this might affect differently the different bands parked along the column.

In order to dampen the pressure shock and reduce the rate at which flow rate and pressure change along the column but particularly at its inlet, we made the following two experiments:

1. The flow rate is progressively decreased to zero and increased back to its constant value, in order to avoid the perturbations of the mobile phase velocity at the column entrance. A linear decrease then increase of the flow rate were programmed with a gradient time of 1.5 min.
2. The Halo HILIC column 2 was inserted upstream the Halo HILIC column 1 and the standard MLPP experiment was carried out, the flow rate being stopped and resumed abruptly. However, the bands were parked only in the downstream, Halo HILIC column 1.

Fig. 9 shows the results of the first series of experiments. The peak parking time was set at 2 h. Despite a very smooth decrease and increase of the flow rate (gradient time 1.5 min) no improvement in the shape of the concentration zone located at $z = 1.5$ cm was observed. Fig. 10 shows the results of the second series of experiments. Interestingly, the anomaly has completely disappeared. Insertion of a second column upstream the column used for parking the bands eliminated the anomaly. This confirms that the anomalies observed are not due to a structural default in the column bed. Dampening the pressure surge and the flow rate perturbations by inserting a column playing the role of a resistor/capacity system between the pump and the column under study eliminated the problem encountered when performing the PP or MLPP experiments with the columns used in this work.

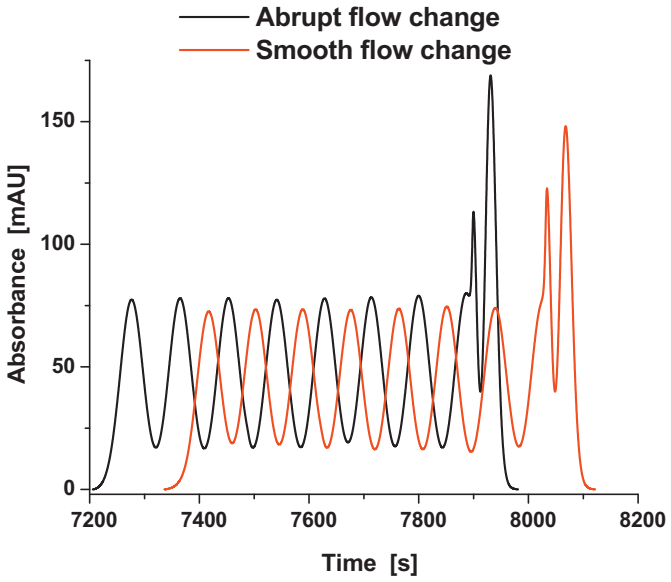

Fig. 9. Comparison between the MLPP chromatograms of uracil when an abrupt and a smooth change in the step flow rate are applied. Same eluent, temperature, flow rate, column, and sample locations as in Fig. 4. A new sample vial was prepared. The smooth change was programmed by setting a linear flow rate gradient from 0.18 mL to 0 mL/min (stop flow) and from 0 to 0.18 mL/min (resume flow) during one and a half minute. The parking time was set at 120 min. Note the expected shift of the chromatograms and the persistence of the band broadening anomaly of the last eluted peak.

Finally, Fig. 11 shows the results of the MLPP method when 18 locations were selected in the chain of the two Halo HILIC columns 1 and 2 (9 locations in each column). The results confirm that the anomaly in the peak shape of the zone parked at the entrance of column 1 should not be of concern. It confirms that the band distortion takes place in the entrance region of the first column of the series.

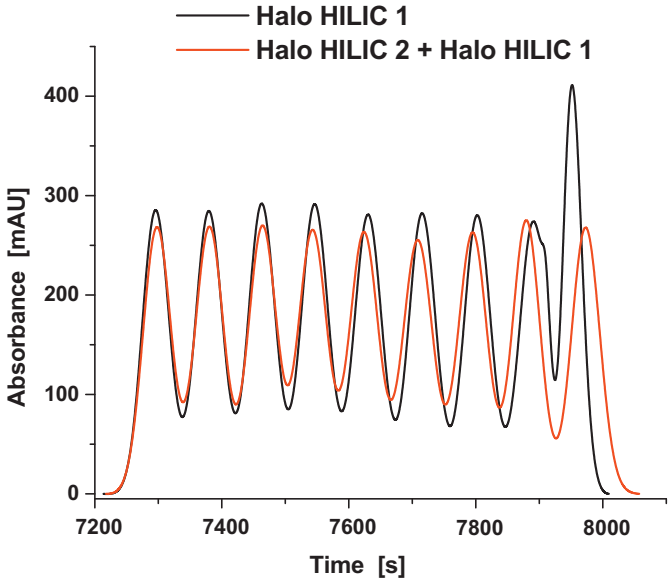

Fig. 10. Comparison between the MLPP chromatograms of uracil between the standard procedure and when a second column has been placed upstream the column under investigation. Same eluent, temperature, flow rate, column, and sample locations as in Fig. 4. Sample solution as in Fig. 9. The parking time was set at 120 min. Note the elimination of the band broadening anomaly of the last eluted peak.

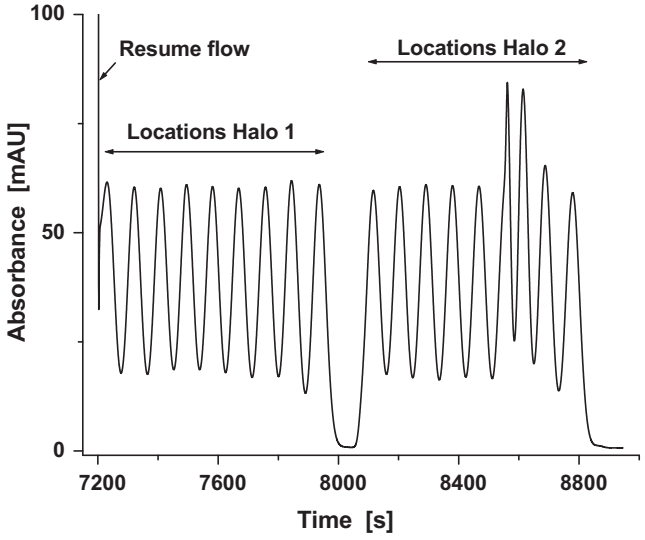

Fig. 11. MLPP chromatograms recorded when a second column (column 2) was placed upstream the investigated column (column 1). Same experimental conditions as in Fig. 10, except 18 locations were selected (9 in column 2 + 9 in column 1). Note that the band broadening anomaly usually observed in absence of column 2 and related to the last eluted peak zone in column 1 vanishes. Yet, this anomaly now pops out in the peak zones 2–4 in the first half-length of column 2.

5. Conclusion

This work demonstrates that the PP method should be used cautiously. Extension of the conventional PP method, which injects a single band into the column and parks it in a single location where axial diffusion is measured, to the MLPP method, which injects several bands parked in different locations spread along the column, so axial diffusion can be measured in different places, allows the detection of possible anomalies in the axial diffusion of the different bands at specific points in the column.

Most surprisingly, use of the MLPP method revealed that the band widths of concentration profiles located in the entrance region of the column (within 10–20% of the total column length) are much narrower and more distorted than those of most zones after diffusion times larger than a few hours. Complementary experiments show that these anomalies can be eliminated if a flow resistance (a second column for example) is placed between the pump and the column. Finally, the MLPP method showed that diffusion parameters derived from the conventional PP method are nearly identical everywhere else along well packed chromatographic column.

MLPP is a useful tool that prevents analysts from deriving erroneous longitudinal diffusion coefficients (the B coefficient in the reduced HETP plots) from the broadening of single bands parked in arbitrarily selected location in the standard PP method. A simple guard column with a flow resistance equivalent to that of the column under investigation should be used to solve this problem.

The influence of several experimental factors such as the nature of the probe compound (and its retention factor) and of the chromatographic mode (RPLC, IEX, ...) on the MLPP observations also need to be investigated. One may want to select a rather retained compound for the development and for investigation of the method to park a large number of bands along the column in MLPP experiments, because it would be important to confirm the existence of anomalies in the static diffusion of samples in other chromatographic modes than HILIC.

Finally, one may want to extend the use of the peak parking method from liquid chromatography to supercritical fluid chromatography. Since the viscosity of supercritical carbon dioxide is much smaller (ca. one order of magnitude) than that of the conventional eluents used in LC, our results suggest that some serious difficulties might arise if adequate experimental precautions are not considered. MLPP could serve as a powerful tool to check whether static band dispersion takes place normally between the inlet and the outlet of the SFC column.

Acknowledgements

This work was supported in part by the cooperative agreement between the University of Tennessee and the Oak Ridge National Laboratory. We thank Jack Kirkland and Joseph di Stefano (Advanced Material Technologies, Wilmington, DE, USA), Jerry Wang (Agela Technologies, Newark, DE, USA), and Tivadar Farkas (Phenomenex, Torrance, CA, USA) for the generous gifts of the Halo, Venusil, Luna-diol and Kinetex HILIC columns, respectively, used in this work and for their fruitful discussions.

References

[1] J.H. Knox, L. McLaren, Anal. Chem. 36 (1964) 1477.
[2] J. Knox, H. Scott, J. Chromatogr. 282 (1983) 297.
[3] F. Gritti, G. Guiochon, Chem. Eng. Sci. 61 (2006) 7636.
[4] F. Gritti, G. Guiochon, AIChE J. 57 (2011) 333–345.
[5] K. Miyabe, Y. Matsumoto, G. Guiochon, Anal. Chem. 79 (2007) 1970.
[6] K. Miyabe, G. Guiochon, J. Chromatogr. A 1217 (2010) 3053.
[7] F. Gritti, G. Guiochon, Anal. Chem. 79 (2007) 3188.
[8] K. Miyabe, N. Ando, G. Guiochon, J. Chromatogr. A 1216 (2009) 4377.
[9] Y. Miyabe, K. Matsumoto, G. Guiochon, Anal. Chem. 65 (2010) 3859.
[10] F. Gritti, G. Guiochon, J. Chromatogr. A 1216 (2009) 4752.
[11] F. Gritti, I. Leonardis, J. Abia, G. Guiochon, J. Chromatogr. A 1217 (2010) 3219.
[12] F. Gritti, G. Guiochon, J. Chromatogr. A 1218 (2011) 907–921.
[13] F. Gritti, G. Guiochon, AIChE J. 57 (2011) 346–358.
[14] F. Gritti, G. Guiochon, J. Chromatogr. A 1217 (2010) 5137.
[15] F.C. Leinweber, M. Pfafferodt, A. Seidel-Morgernstern, U. Tallarek, Anal. Chem. 77 (2005) 5839.
[16] M.C. Stone, G. Carta, J. Chromatogr. A 1160 (2007) 206.
[17] T.E. Bankston, M.C. Stone, G. Carta, J. Chromatogr. A 1188 (2008) 242.
[18] F. Gritti, G. Guiochon, J. Chromatogr. A 1217 (2010) 8167–8180.
[19] F. Gritti, G. Guiochon, Chem. Eng. Sci. 65 (2010) 6327.
[20] K. Miyabe, Y. Kawaguchi, G. Guiochon, J. Chromatogr. A 1217 (2010) 3053.
[21] E. Wilson, C. Geankoplis, J. Ind. Eng. Chem. (Fundam.) 5 (1966) 9.
[22] C. Wilke, P. Chang, AIChE J. 1 (1955) 264–270.
[23] F. Gritti, G. Guiochon, J. Chromatogr. A, submitted for publication.
[24] P. Horng, M.R. Brindza, R.A. Walker, J.T. Fourkas, J. Phys. Chem. C 114 (2010) 394.